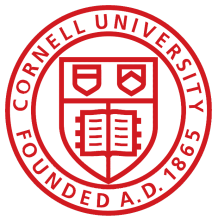

Cornell University

Can You Take the Heat?
Model of Temperature and Neuronal Membrane Potential Changes in the Brain Tissue due to Deep Brain Stimulation

Keywords: Deep Brain Stimulation (DBS), COMSOL, Temperature, Membrane Potential

BEE/MAE 4530: Computer Aided Engineering

Authors: Cole Dawson, Ana Paula López Guerrero Díaz, Devanshi Jain, Tooba Subhani

Table of Contents

1. Executive Summary

In the world, millions of people live with neurological conditions such as epilepsy, Parkinson's or major depression disorder (MDD). As a viable treatment for their symptoms, Deep Brain Stimulation (DBS) was created. This medical procedure involves a surgery where a magnetic probe (neurostimulator) is implanted into a specific region of the brain. There, the electrodes in the probe produce electromagnetic pulses to regulate neuronal activity. Albeit this is a verified and reliable procedure, many unknowns arise from DBS; such as the extent of neuronal activity alterations due to the increase of brain temperature due to electromagnetic stimulation.

Hence, the objective of this project is to simulate in COMSOL how DBS can influence the brain tissue in terms of temperature variation and neuronal activation. A 2D model of the thalamic and hypothalamic regions of the brain in contact with the DBS probe was created. The model solved the bioheat equation, the Laplace equation for the voltage of the electrodes, the Nernst equation and Hodgkin-Huxley equation for the membrane potential. To attain an accurate model, the process of validation, verification, mesh convergence and sensitivity analysis were also conducted and included in the paper.

The results of the model provided insights on how heat transfer takes place from the probe to the thalamus and the hypothalamus as a result of electrical heating. Essentially, the change in temperature in the tissues considering a point 0.01 mm away from the electrode was of 0.0055 ºC in the thalamic region (starting from the initial temperature of 38.5 ºC in the brain, to 38.5055 ºC), whereas in the hypothalamic region it was 0.0048 ºC (where the peak temperature was 38.5048 ºC), after 1 second of heating. The same analysis was performed for a point 0.73 mm away from the electrode and the temperature change was 0.0023 ºC and 0.0020 ºC for the thalamic and hypothalamic regions respectively. When extended to a minute, the thalamus increased in temperature by around 0.042 ºC. The increase in temperature did not exceed 1 ºC, and thus, it can be inferred that the temperature change was optimal. This was validated by a study made by Elwassif et al., where they modeled a brain temperature increase of nearly 0.8 °C after 15 minutes during DBS. Approximating this rate for 1 minute gives a temperature increase of 0.053 ºC, exceeding the 0.042 ºC observed at the point 0.73 mm away from the electrodes. Additionally, considering that same point, the membrane potential sharply increases from -70 mV, which is the resting membrane potential, all the way to +25 mV. The closer point's membrane potential experienced an increase to +60 mV, which is the maximum action potential. The membrane potential at both points then continues to periodically oscillate between -35 mV and either +25 or +60 mV, respectively. This oscillation is closely mimicking the changes in membrane potential during normal neuronal activity.

The temperature and membrane potential trend with varying distance (along a line), in the tissue domain was also observed, exhibiting expected trends of reduction in values with increasing distance from the electrodes with the highest temperature for the thalamic region being 38.5055 ºC and that for the hypothalamic region being 38.5048 ºC after 1 second of stimulation. The membrane potential along an arc in the tissue domain shows a gradual decrease with a maximum value of 60 mV near the electrode and -35 mV at a distance of 10 mm from the electrode. As both temperature and membrane potential values are directly influenced by the voltage from the electrodes, the trend of the 1.8 V pulse sent by the electrode over distance was also assessed. The voltages at 0.01 mm, 0.73 mm, and 6.73 mm from the electrode were found to be 1.8 V, 1.15 V and 0.15 V respectively.

Conclusively, the simulation supports the notion that the voltage from the DBS procedure does have an effect on increasing the temperature and the membrane potential of the brain. These results are significant because DBS can induce a high amount of heat accumulation over time in patients who have undergone the procedure, which can also cause serious side effects which may impact brain function. The results of this study welcome further investigation and this can be done by examining modifications in probe features and placement of electrodes to maximize efficiency and reduce overall increase in brain temperature. A study can also be performed to understand the kind of changes induced in the tissue microenvironment due to increase in temperature. Understanding the dynamics of heat transfer can help estimate which regions of the brain can be highly impacted and how this can be mitigated.

2. Introduction

Up to this day, neurological conditions are still one of the main unresolved dilemmas in the medical world. Some widely known neurological conditions are epilepsy, Parkinson's disease and major depressive disorder. Globally, one out of 26 people are diagnosed with epilepsy (150,000 americans each year), approximately 280 million people have major depression disorder (MDD), and over 10,000 million people live with Parkinson's [1]. These conditions often develop due to some loss of neuronal activity and thus do not deliver their required function. As a viable method of treatment for these cases, the Deep Brain Stimulation (DBS) procedure was created. In this medical procedure, a magnetic probe is implanted into the brain, where it sends electromagnetic signals to directly stimulate neuronal activity and regulate the symptoms of most movement and neuropsychiatric disorders. The amount of electromagnetic stimulation is controlled by a pacemaker-like device placed in the upper chest (traditionally, it is externally controlled). DBS was first introduced in France in 1987 [1], and in 2002 it was granted approval by the US Food and Drug Administration (FDA) for the treatment of Parkinson's disease [2].

The thalamus and hypothalamus are the primary regions of the brain where the probe is inserted and that DBS has an effect on. These parts of the brain work as the information relay system and processes all information related to body senses (except smell) before passing it to the cerebral cortex for interpretation and further response. The thalamus is also responsible for sleep, wakefulness, consciousness, learning and memory. Any damage in the thalamic structures can lead to movement disorders. Thalamic DBS has been proven advantageous for the treatment of drug-resistant epilepsy. In this project, it is hoped that the study of the stimulation effects and heat diffusion on these different layers will be effectively obtained.

Homeostasis in the human body is a crucial function to support cellular growth and survival. Especially in the brain, any minor changes in temperature will directly affect these processes. Extended temperature change can also affect brain chemistry and can lead to unexpected complications. Although current (I) and temperature (T) are not directly related to the outcome of the DBS procedure, transfer of current through any material which provides resistance will result in temperature increase. That is the reason why this paper has the objective to identify to what extent temperature varies in the brain due to DBS, and if it does, what effects it poses on neuronal activity (and if it is significant enough to induce long term damage).

In a research developed by Elwassif et al. on the temperature change due to deep brain stimulation, they reached the conclusion that temperature on the surrounding tissue will increase by around 0.8 °C over the course of 15 minutes (depending on the stimulation/tissue parameters). Because changes in brain temperature are a delicate matter, for this project the intention will be not to surpass that set temperature or rate. If it is exceeded, the result would represent a sign that major changes need to be made to how DBS is administered, as even a 0.8 °C increase in the brain is alarming.

In this study, the effect of DBS on the surrounding tissue will be assessed first, along with how significant the temperature change is. The bioheat model will be employed in two particular layers of the brain - the thalamus and hypothalamus - to assess temperature change with constant volumetric blood flow. The geometry of the probe will be simplified using a 2D axisymmetric model. The second priority is to understand how temperature induced changes in the neuronal tissue are affecting membrane potential of neurons and the signal transduction. Neuronal activation is fundamentally explained by the Hodgkin-Huxley model, a conductance based model which describes how action potentials are initiated and propagated in a neuron. Although the Hodgkin-Huxley model will not be used directly, a neuron model which is based on it will be employed in order to assess thalamic neuronal activation characteristics. This neuron model will allow the finding of the change in the membrane potential with respect to time due to the electromagnetic signals emitted by the probe and the temperature change in the tissue.

The DBS lead model 3389 developed by Medtronic will be studied. The probe is 13.5 mm long and consists of 2 electrodes, both 1.5 mm in length with 0.5 mm spacing. The Implantable Pulse Generator (IPG) controls the power supply and pulse delivery for the DBS lead, and is variable depending on the indication for which DBS is being used for treatment. It is the programmable element of the DBS system that modulates parameters like the pulse width, frequency, and duration. The Medtronic 3389 DBS System produces monopolar stimulation that generates a spherical electrical field that radially diffuses into the tissue from the electrode-tissue interface.

3. Problem Statement

DBS is considered a pioneering therapeutic procedure for diseases that impact brain function. As electrical impulses are generated by the electrode at a set frequency depending on the indication, they help regulate abnormal electrical activity that is generated by the brain in the diseased state. However, generation of these electrical impulses is accompanied by heat generation at the electrode-tissue interface that continues to diffuse through the brain tissue. As per a study conducted by Elwassif et al., brain temperature increases by nearly 0.8 °C over the course of 15 minutes during DBS, and is a function of the stimulation parameters. While the average brain temperature is higher than the regular body temperature (around 38.5 °C), any increment in brain tissue temperature can aggressively deteriorate nerve fibers and hinder brain activity. In this study, the simulation of how a DBS electrode can lead to heat dissipation through the thalamic tissue and the hypothalamic tissue during stimulation, and how it may affect membrane potential through neuronal activation, will be analyzed.

4. Design Objectives

The goal of this simulation is to analyze to what extent the temperature of the tissue surrounding the DBS probe increases due to the pulses it emanates. It is predicted the temperature will increase by around 0.8 °C, or 1.4 °F, which is a significant increase. Additionally, comments on the area of the electrode interfacing the brain tissue and its impact on heat generation will be made.

Moreover, temperature induced changes in the membrane potential of a neuron lying in the thalamic/hypothalamic region will be evaluated. The potential of the neurons closest to the electrodes is expected to increase from -70 mV to around +40 mV, based on the increase in potential that neurons typically experience from an action potential. This extension will help in the formulation of an in-depth analysis of changes in signal transmission through a neuron during DBS.

5. Visual Representation and Schematic

In order to design the schematic, the layers of the brain that were considered for the model were the thalamus and the hypothalamus. The following figure ***(Figure 1)*** shows an illustration of the layers of the brain in order to provide a clearer visualization of the structure and the location of the probe inserted. Beneath it, the actual schematic is pictured (which includes the two layers of the brain previously mentioned and the probe) that will be computed into COMSOL:

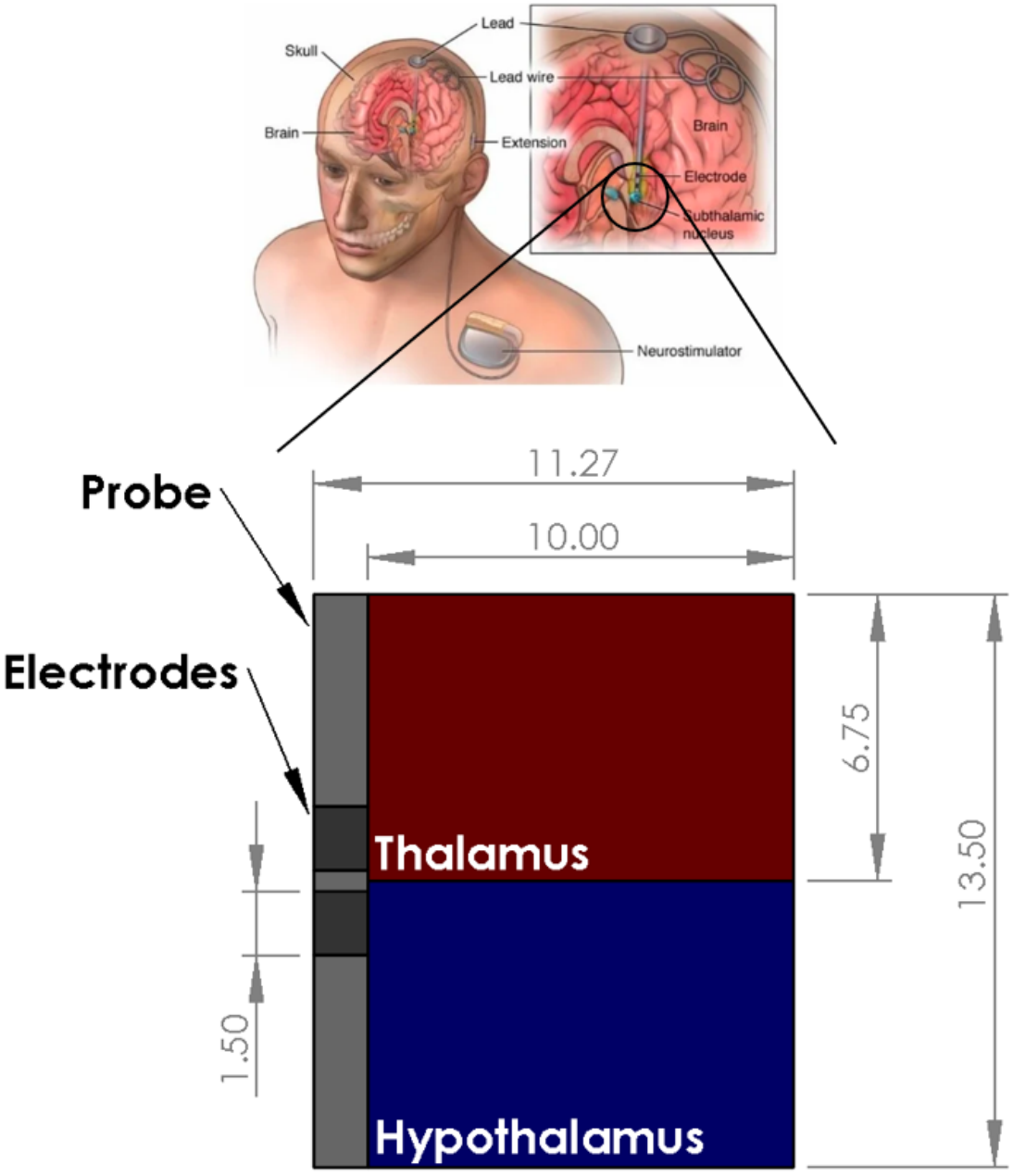

Figure 1: Concept of deep-brain stimulation (DBS). Pictured on top is the probe within the brain, and on the bottom is a schematic of the measurements of the probe and adjacent brain tissue. All dimensions are in millimeters (mm).
Electronics ***2022****, 11(6), 939;* ***https://doi.org/10.3390/electronics11060939***

As shown in ***Figure 1***, the pulse generator is planted in the chest and the probe connected to it is surgically implanted in the region of the brain to be targeted. This probe sends out electrical signals which stimulate the surrounding tissue, which, in the case of the brain, is a cluster of neurons. The geometry was developed keeping in mind that the thalamus and hypothalamus are neighboring regions of the brain and the most targeted areas for DBS treatments. As joule heat is produced in any electrical field where the electrical currents are circulating, we're developing this model to study temperature changes induced by the heat produced in the tissue. These temperature changes also affect the membrane potential of a neuron

which helps the propagation of a signal through the neuron. Changes in temperature alter the speed and frequency of signal transmission; hence, we're extending our model to study temperature induced changes in the membrane potential.

6. Mathematical Assumptions and Possible Sources of Error

The governing equations and boundary conditions that will be presented in the following sections were made under certain assumptions. These assumptions are:

1. The geometry will be approximated as a 2D axisymmetric cylinder.
2. Conduction will be analyzed between each layer of the tissue, as well as between the electrodes and the tissue.
3. The domain of the brain tissue is considered large relative to the probe.
4. Resembling the actual experimental DBS process, the scope of the problem in the model is limited to a particular region of the hypothalamus and the thalamus that is directly interfacing and in proximity to the electrodes. For this reason, 2 electrodes on the probe were simulated, with each electrode interfacing with the thalamic and hypothalamic regions respectively. This is beneficial as it leads to a simple computational model.
5. The surface charge density is assumed to be negligible at the boundaries between the probe and layers of tissue.
6. We assume that the probe extends to the height of the thalamus and the hypothalamus, and is in contact with them. However, there are only 2 electrodes on the probe that will be responsible for electrical conduction and thereby, heat generation. The rest of the probe is considered to act as thermal and electrical insulation.
7. As we wanted to observe the difference in temperature trend in the two layers, we chose to use different values of thermal conductivities from the range (0.53 - 0.56) we obtained from the database (ETH Zurich) for tissue properties. Both regions have the same range of thermal conductivities, but due to the hypothalamus playing a larger role in regulating body temperature, we are assuming the value of the thermal conductivity of the hypothalamus to be on the higher end of the range (0.56) and the value for the thalamus to be on the lower end (0.53).
8. Conservation of energy and charge are assumed, allowing the use of the bioheat equation and Maxwell's equations to solve for temperature, voltage and membrane potential. Additional Joule heating develops during electrical stimulation (DBS) as a result of the conversion of electrical energy lost during conductor flow into thermal energy; modeled as $\nabla \cdot (\nabla \sigma V_T)$, with V_T being the local potential induced by simulation.

7. Governing Equations

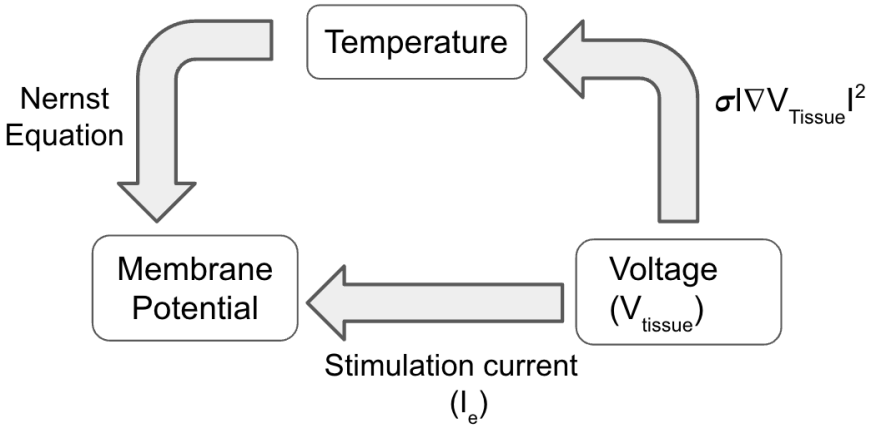

Figure 2: Image of the dependency between voltage, temperature and membrane potential; showing the connection between the governing equations.

The first governing equation the model implements is the bioheat equation, which describes the temperature change in the brain due to DBS:

$$\underbrace{\rho c_p \frac{\partial T}{\partial t}}_{change\ in\ storage} = \underbrace{k\nabla^2 T}_{conduction} + \underbrace{\underbrace{\rho_b w_b c_b (T - T_b)}_{convection\ due\ to\ blood\ flow} + \underbrace{Q_m}_{metabolic\ heat\ generation} + \underbrace{\sigma|\nabla V_T|^2}_{electrical\ heat\ generation}}_{Total\ source\ term} \tag{1}$$

The elements that represent change in storage, conduction, convection due to blood flow, voltage and metabolic heat generation are clearly specified, where T is the temperature [K] of the brain tissue and V_T is the electric potential [V] of the tissue.

V_T is described by solving the Laplace equation:

$$\nabla \cdot (\nabla \sigma V_T) = 0 \tag{2}$$

Table 1: Parameters for equations (1) and (2).

Symbol	Description	Value	Dimension
k	Thermal conductivity of brain tissue	$0.5 - 0.6$	W/(m·ºC)
ρ	Density of the brain tissue	1040	kg/m^3
c_p	Specific heat capacity of the brain tissue	3650	J/(kg·ºC)
σ	Electrical conductivity	$0.15 - 0.35$	S/m

ρ_b	Density of the blood	1057	kg/m^3
w_b	Volumetric blood perfusion rate per unit volume	$0.004 - 0.012$	mL/s/mL
c_b	Specific heat of blood	3600	J/(kg·ºC)
T_b	Brain core temperature	38.5	ºC
Q_m	Metabolic heat source	0	It is assumed that $Q_m = 0$ in this paper.

The second governing equation that will be solved is the Hodgkin-Huxley model. A significant part of the model is the Nernst Equation. The Nernst equation is a cornerstone of our project as its terms calculate the concentration of K^+, Na^+, and Cl^- ions. The reason why this is crucial is because the rate of flux of these ions causes potential of the membrane to increase or decrease, and this potential further governs the firing of signals in the neurons. Further implementing the Hodgkin-Huxley model helps us arrive at an understanding of how membrane potential, V_m, would change with time as a result of increasing temperature. The ionic potentials V_{Na}, V_K, and V_L (the ionic potentials as a result of sodium ions, potassium ions, and chloride ions) are affected by the temperature changes as it has a direct effect on the opening of the ion channels present in the neuronal membrane. This relationship between the ionic potential and temperature will be assessed using the Nernst equation:

$$V_{ion} = \frac{RT}{F} ln \frac{[ion]_i}{[ion]_o} \tag{3}$$

Where V_{ion} is the equilibrium potential [V] for K^+, Na^+, and Cl^- and T is the absolute temperature [K].

Table 2: Parameters for equation (3).

Symbol	Description	Value	Dimension
R	Universal gas constant	8.3144598	J/(mol·K)
F	Faraday's constant	96,485	C/mol
$[ion]_i$	Intracellular concentration of a specific ion	0.150 (K) 0.015 (Na) 0.010 (Cl)	M or mol/L
$[ion]_o$	Extracellular concentration of a specific ion	0.005 (K) 0.150 (Na) 0.110 (Cl)	M or mol/L

The Nernst equation provides the values for V_{Na}, V_K, and V_{Cl} and introduces the concept of temperature dependence on ion channels [9]. The Hodgkin-Huxley model is then introduced with these

values as follows as a function of the time-dependent membrane potential. As the concentration of Na^+, K^+, and Cl^- ions changes, it impacts the rate at which the ion channels operate and neurons fire signals, hence increasing the resting membrane potential to action potential, which helps in propagating the signal [10]:

$$\underbrace{C_m \frac{dV_m}{dt}}_{membrane\ potential} = \underbrace{-\bar{g}_{Na} m^3 h}_{Na\ channel\ conduction} (V_m - V_{Na}) \underbrace{-\bar{g}_K n^4}_{K\ channel\ conduction} (V_m - V_K) \underbrace{-\bar{g}_{Cl}(V_m - V_{Cl})}_{leak\ current} + \underbrace{I_e}_{stimulation\ current} \tag{4}$$

I_e, the stimulation current, can be found using the formula:

$$I_e = \sigma \frac{\nabla V_T}{d} \tag{5}$$

Here, the leak current mainly comprises chloride ions. The terms n, m and h demonstrate the probability of open and closed channels for potassium and sodium respectively, which can be extrapolated from the temperature dependence graph. The stimulation current represents the effect that the change in voltage has on the membrane potential.

Table 3: The values for the respective terms for equations (4) and (5).

Symbol	Description	Value	Dimension
C_m	Membrane capacity	0.001	mF/cm^2
$\bar{g}_{Na}$	Maximum conduction of sodium channel	120	mS/cm^2
$\bar{g}_K$	Maximum conduction of potassium channel	36	mS/cm^2
$\bar{g}_{Cl}$	Maximum conduction of chloride channel	0.33	mS/cm^2
σ_T	Electrical conductivity of the Thalamus tissue	4.75	mS/cm
σ_H	Electrical conductivity of the Hypothalamus tissue	4.19	mS/cm

8. Boundary and Initial Conditions

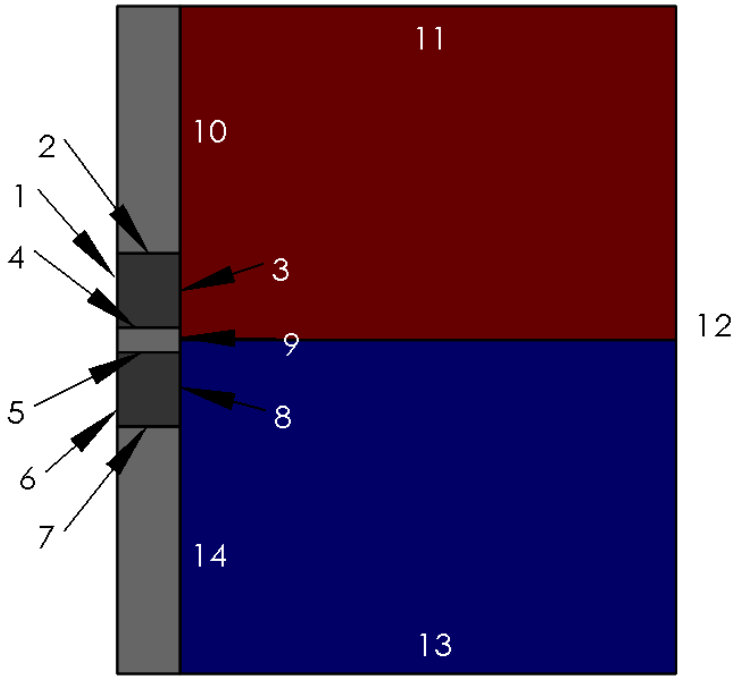

Figure 3: Schematic of probe with labeled boundaries.

8.1 Thermal Boundary Conditions

The domain was considered to be only the tissue and the electrodes, with the rest of the probe being excluded due to the change in temperature in those regions not being important to the study. A zero flux boundary condition was set for boundaries 11 and 13 due to them being a large distance from the probe. The boundaries 2, 4, 5, 7, 9, 10 and 14 are considered to have a zero flux boundary condition due to being in contact with the non-electrode parts of the probe, which is assumed to be unaffected by the electromagnetic waves from the electrodes. Boundaries 1 and 6 have zero heat flux due to symmetry. Boundary 12 is a large distance from the probe, so it is set at a constant temperature of 38.5 °C. This is normal brain temperature.

8.2 Electrical Boundary Conditions

For the electrical boundary conditions, the probe as a whole was excluded from the domain, as the electric potential of the probe is irrelevant to the study. It is assumed boundaries 11, 12 and 13 are grounded due to being a large distance from the electromagnetic waves of the probe. At boundaries 9, 10 and 14, the boundary condition is assumed to be zero electrical flux. At boundaries 3 and 8, an electric potential condition of 1.8 V is placed to act as the source of the electromagnetic waves that propagate throughout the tissue.

8.3 Initial Conditions

For the initial conditions, the brain tissue will be assumed to be at its standard temperature of 38.5 ºC before the probe begins sending out electrical signals.

9. Time Stepping

As per the bioheat simulation model of DBS developed by Elwassif et al. [4], the total duration of the voltage pulse was considered to be 108.8 μs, with 5800 μs between each pulse [15]. The time-step that was decided upon was 59.088 μs, which is the value of one hundredth of the period. If a time step smaller than this one is used, the simulation is likely to eventually encounter an error and crash. On the other hand, even though increasing the time step makes the simulation more stable, it is less precise. This in turn makes the resting period either less accurate or absent completely. Regardless of the time step used, the convergence plot would have at least one spike in the reciprocal of the step size out of nowhere. By choosing the stipulated time step, a more realistic solution was achieved, allowing COMSOL to run without crashing. Also, this new time-step provided sufficient duration to create an accurate model where temperature changes caused by DBS could be clearly identified. The range decided was 1 second, as even a simulation for a time this short takes over an hour and a half to run. This 1 second period still provides an accurate representation of the trends that can be expected to see as time progresses, however, considering that on a daily basis a patient undergoing this treatment receives longer and constant pulsations of DBS throughout the day. A single 60 second simulation was run in the thalamus in order to analyze trends in the temperature and membrane potential over longer periods of time.

10. Results

10.1 Complete Solution

For the complete simulation, a periodic piecewise function for voltage was run. The voltage source was 1.8 V for 101.8 μs, with 5800 μs between each pulse. During the periods where there are consistent spikes in the voltage and membrane potential, the simulation performs as expected, with a sudden spike followed by a short rest period before another spike. The membrane potential behaves extremely similar to an action potential. The temperature increases slightly during each pulse, before plateauing and eventually decreasing before the next pulse, leading to a general upwards trend. The simulation was run for a period of 1 second with the above-mentioned boundary, initial, and domain conditions. Ultimately, a complete solution describing the variation of temperature and membrane potential throughout the area of the thalamus and hypothalamus during the DBS procedure was achieved.

10.2 Variation of temperature and membrane potential in point of interest 0.01 mm away from the electrode

To understand the temperature and membrane potential variations in the thalamic and hypothalamic regions, a point of interest in each region was selected and variance in temperature and membrane potential was further analyzed. First, a point was considered in the thalamic and hypothalamic regions such that it was nearly in contact with the electrodes:

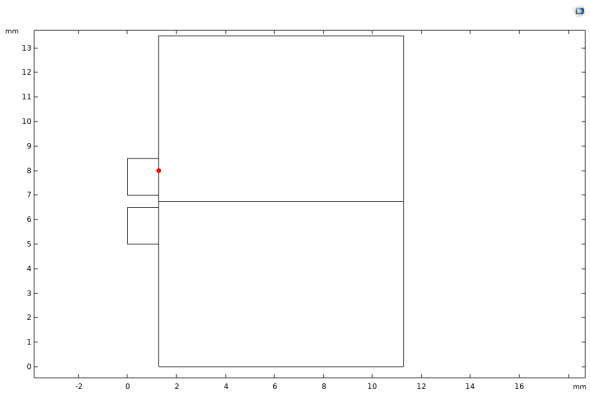
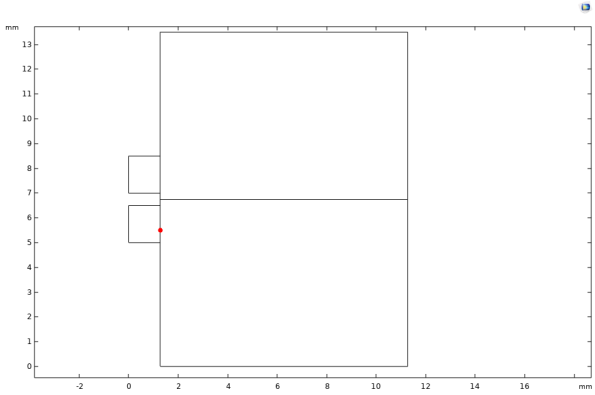

Figures 4 and 5: Graphs with the geometry along with the point of interest in the thalamic and hypothalamic regions, 0.01 mm away from the electrode.

Then, the variance of temperature in the point at the thalamus and hypothalamus was plotted for the total simulation time of 1 second. The variance in membrane potential for a period of 0.03 seconds was plotted as well:

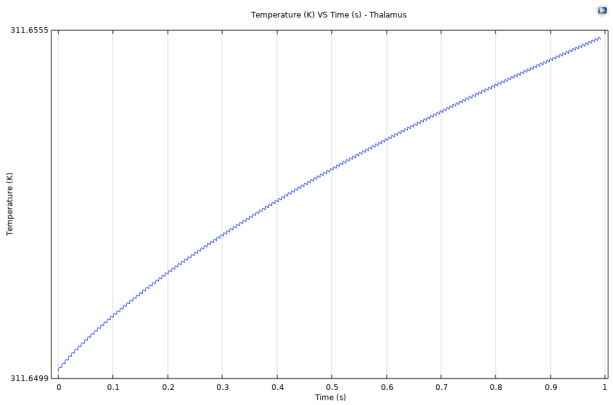

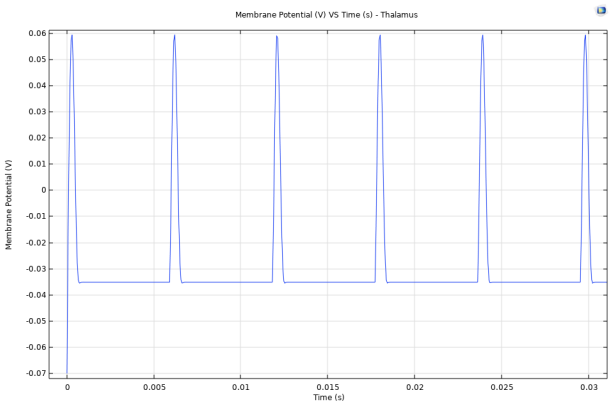

Figures 6 and 7: Graphs showing the temperature and membrane potential variation of the point of interest 0.01 mm away in the thalamic region of the brain.

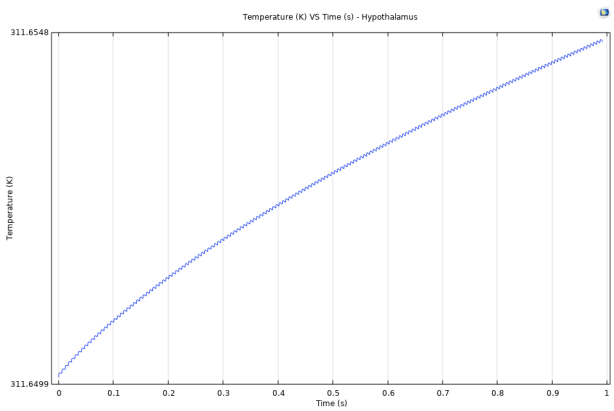

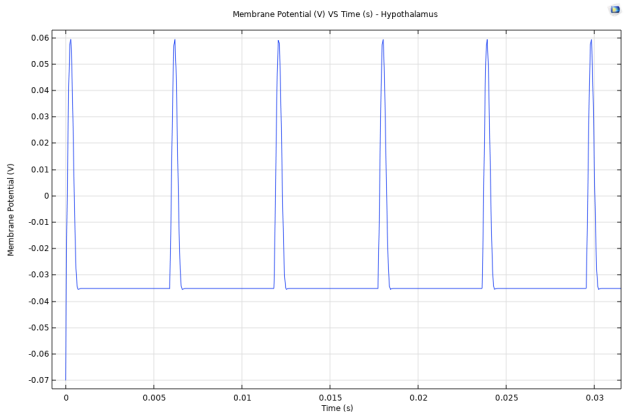

Figures 8 and 9: Graphs showing the temperature and membrane potential variation of the point of interest 0.01 mm away in the hypothalamic region of the brain.

Considering the initial temperature of 38.5 ºC (311.65 K) in the brain, the temperature in the thalamic region increases up to 38.5055 ºC (311.6555 K), whereas in the hypothalamic region the peak temperature is 38.5048 ºC (311.6548 K). As a general trend, the temperature curves for both of the regions seem to follow somewhat of a slight upward trend initially before either beginning to plateau or continuing to increase linearly. This is most probably due to the sudden increase in the temperature as a result of DBS pulsations and consequent increase in voltage in the tissue.

In terms of membrane potential variance, the potential sharply increases from -70 mV, which is the resting membrane potential, all the way to +60 mV, which is the maximum action potential. It then continues to periodically oscillate between -35 mV and +60 mV. This is due to the periodic external voltage from the DBS electrodes, which causes the membrane potential in the neurons to cause a rapid rise and fall for the propagation of the signal, mimicking the changes in membrane potential in neurons. The same trend for membrane potential can be perceived in both the thalamic and hypothalamic regions.

10.3 Variation of temperature and membrane potential in point of interest 0.73 mm away from the electrode

Second, a point in the thalamic and hypothalamic regions farther away from the electrodes was considered. It is at a distance of 0.73 mm:

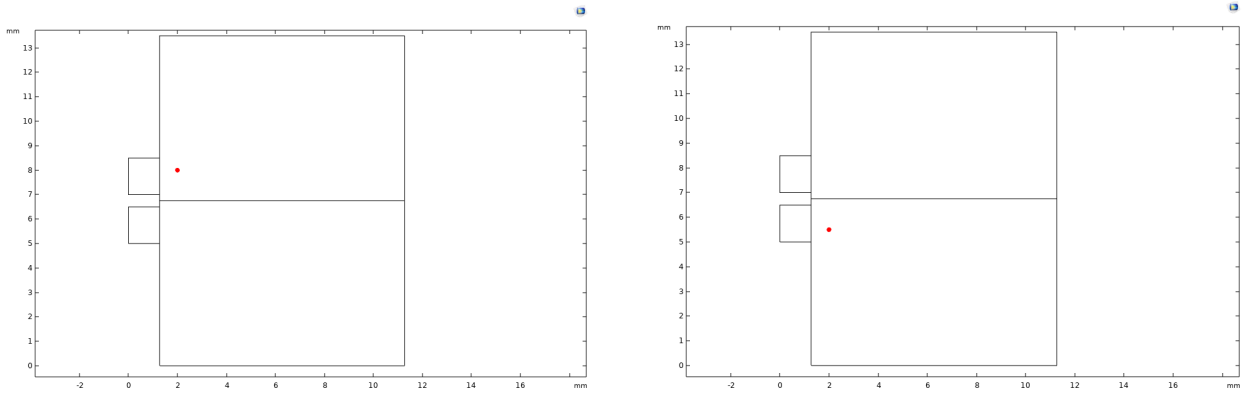

Figures 10 and 11: Graphs with the geometry along with the points of interest in the thalamic and hypothalamic regions, 0.73 mm away from the electrodes

The temperature and membrane potential variation was examined for the point of interest considered in the thalamic and hypothalamic regions (note that the graph on the left reflects the variation in temperature for the total simulation time of 1 second, while the graph on the right shows variation in membrane potential for a period of 0.03 seconds):

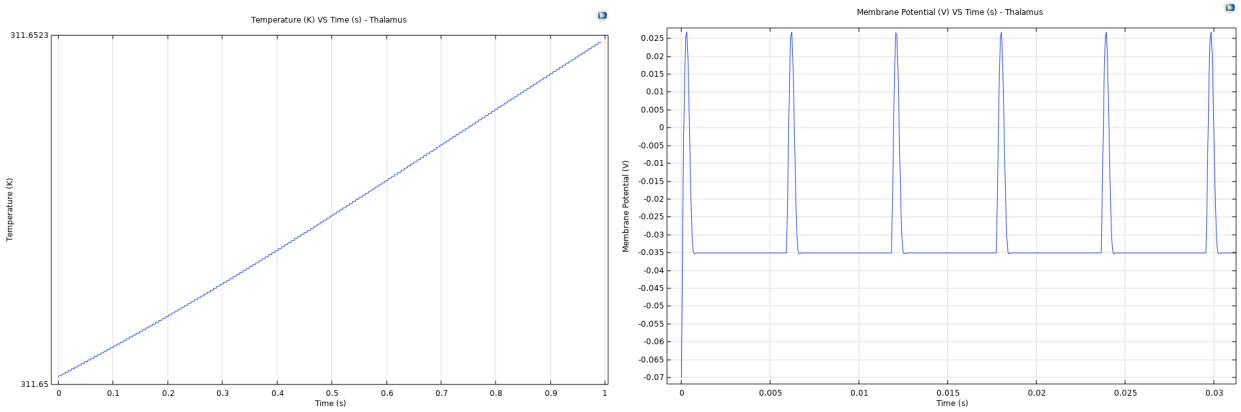

Figures 12 and 13: Graphs showing the temperature and membrane potential variation of the point of interest 0.73 mm away in the thalamic region of the brain.

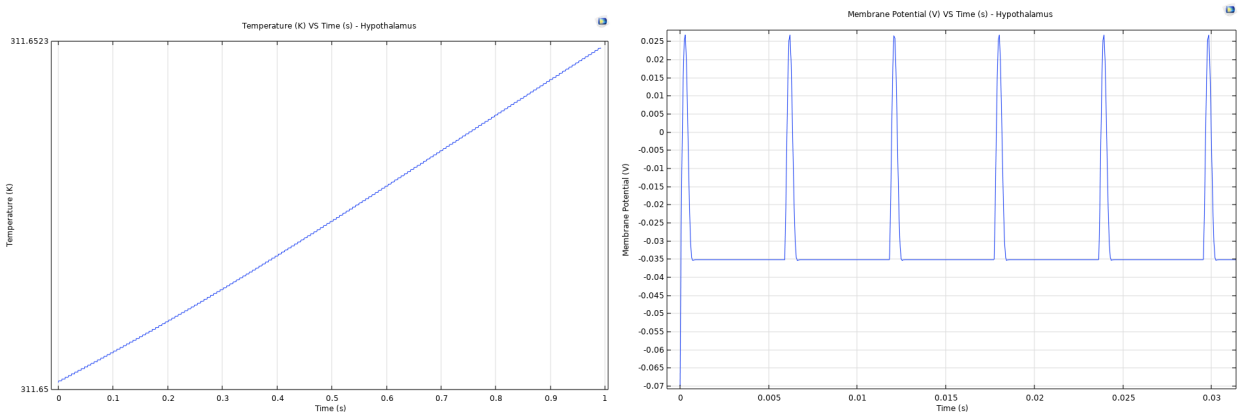

Figures 14 and 15: Graphs showing the temperature and membrane potential variation of the point of interest 0.73 mm away in the hypothalamic region of the brain.

The temperature increases somewhat linearly during the 1 second interval. If the simulation were to continue for a longer period of time, it is predicted that the temperature would continue to increase at a steady rate of approximately 0.0023 ºC/s (or K/s) due to change in temperature from 38.5 ºC (311.65 K) to 38.5023 ºC (311.6523 K). In comparison with ***Figures 7, 8, 9*** and ***10***, where the point of interest was directly in contact with both the regions as well as the electrodes, the peak temperature at this distance (0.73 mm away) is smaller. This indicates that the increase in temperature is localized around the electrode. The difference between the graphs in the two regions appears to solely lie in the difference between their maximum temperatures. While the thalamic region reached a maximum temperature of 38.5023 ºC (311.6523 K) in 1 second, the hypothalamic region only reached a maximum temperature of 38.5020 ºC (311.6520 K). This is surprising, as the thermal conductivity of the hypothalamus was assumed to be greater than the thalamus, leading to the expected conclusion that the hypothalamus would have a greater change in temperature. However, the results of the complete solution debunk this hypothesis. A possible explanation could be the difference in electrical conductivity between the thalamus and hypothalamus. The thalamic layer has a significantly higher electrical conductivity than the hypothalamic layer, which likely suggests higher electromagnetic heating around that area, and thus a higher temperature range.

The membrane potential increases very sharply from -70 mV to +25 mV, before oscillating between -35 mV and +25 mV. This likely occurs because the voltage causes an action potential in the neurons, spiking their membrane potentials each time a pulse occurs. Additionally, there is a short rest period after the membrane potential decreases and reaches the resting membrane potential of -35 mV before spiking again, mimicking the behavior of action potentials.

10.4 Variation of temperature and membrane in a line

Lastly, it was investigated how temperature and membrane potential vary along a single line that runs through the thalamic and hypothalamic regions:

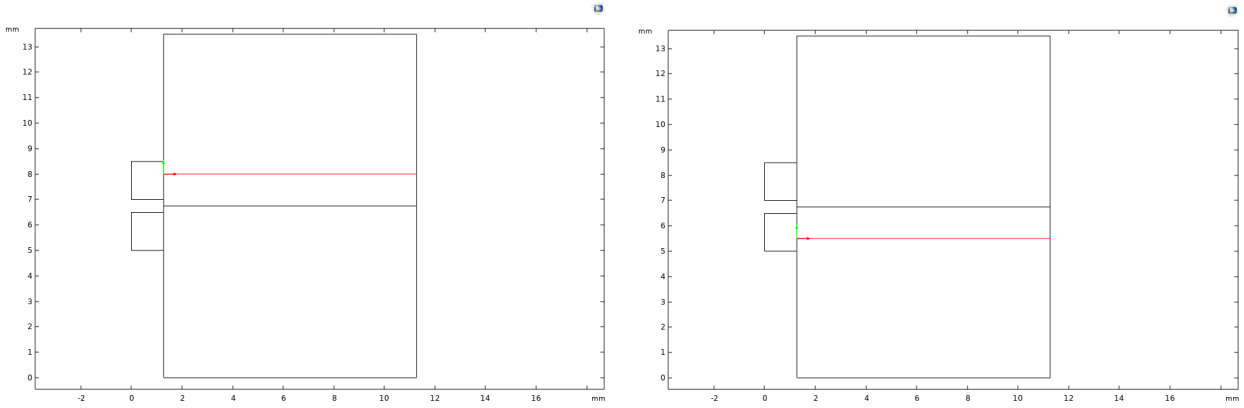

Figures 16 and 17: Graphs with the geometry along with the line of interest in the thalamic and hypothalamic region.

The following plots show the variance of temperature along the line of interest in the thalamic region (on the left) and the hypothalamic region (on the right):

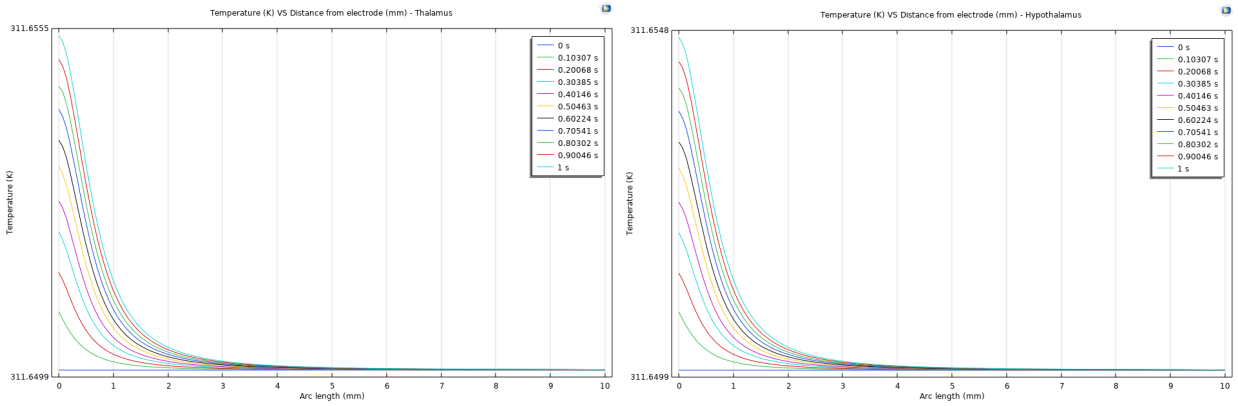

Figures 18 and 19: Plots of the variance of temperature in contrast to the arc length. The different colored lines represent the values at different times (see legends in the graphs). Note that the higher temperature range differs for both of the regions: The highest temperature for the thalamic region is 311.6555 K, while that for the hypothalamic region is 311.6548 K.

When comparing these plots, one can arrive at similar conclusions as the ones stated for the previous plots where the temperature and membrane potential vary over time in a point of interest. Even though in this case the analysis is based on the change of temperature and membrane potential along a

single line, the main change also appears to be the difference between the maximum temperatures, which in the case of the thalamus is 38.5055 ºC (311.6555 K) and for the hypothalamus is 38.5048 ºC (311.6548 K). The temperature near the electrode in the thalamic layer is higher, which wasn't an expected result as the thermal conductivity of the hypothalamus is slightly higher than the thalamic region. One possible explanation for this result, similar to the point analysis, is the difference in the electrical conductivities for each of the layers.

Furthermore, the following plots show the variance of maximum membrane potential along the line of interest in the thalamic region (on the left) and the hypothalamic region (on the right):

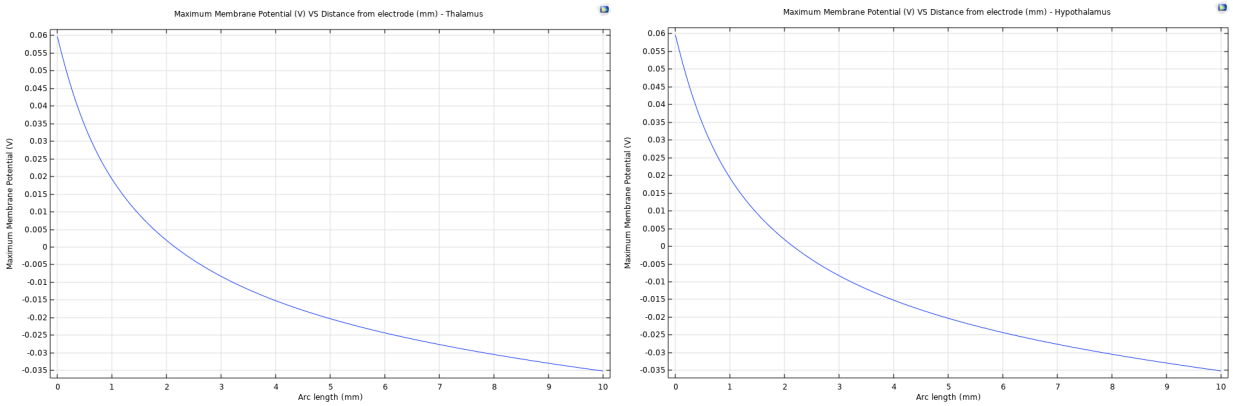

Figures 20 and 21: Plots showing the variance of membrane potential versus the arc length.

The membrane potential values reach a maximum of 0.060 V (or 60 mV, maximum action potential) at the arc length of 0 mm for both the thalamic and hypothalamic regions of the brain, which is the point where the regions are in contact with the electrodes. However, moving away from the electrodes, the membrane potential decreases with distance. As shown in the plots, the membrane potential lowers to -0.035 V (-35 mV) in the arc length of 10 mm with constant periodic input voltage.

10.5 Voltage pulse variation with distance

In addition, we wanted to investigate how the voltage pulse from the electrode varies with distance:

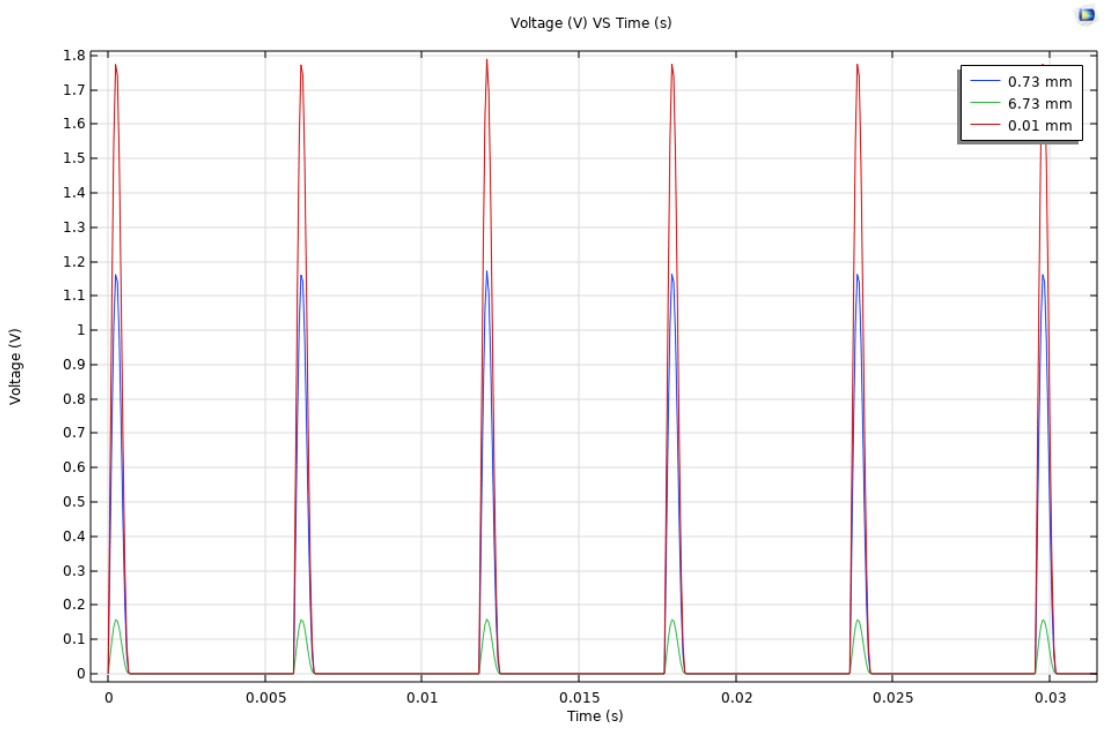

Figure 22: Voltage at distances of 0.01 mm, 0.73 mm, and 6.73 mm from the electrodes.

The figure shows that while a pulse of 1.8 V is sent from the electrode to the tissue, it further decreases as the distance from the electrode increases. The plot oscillates very sharply due to the pulse of 1.8 V that occurs every 5.9088 ms, increasing to 1.15 V at a distance of 0.73 mm before decreasing back down to 0 V periodically. At a point further from the electrodes at a distance of 6.73 mm, it can be seen that the voltage is significantly lower, reaching only 0.15 V after each pulse. This means that a voltage source of only about 0.15 V is available for spiking the membrane potential of the neurons. This was also evident from the point graphs listed above as it can be noticed that the membrane potential decreases with an increase in distance away from the electrode in the tissue.

This is interesting, as it further gives an insight on the DBS procedure and electrode design: The design of the electrodes for DBS differ according to the disease and its indications. For diseases like Parkinson's disease, where one would desire a much higher membrane potential in neurons - high enough to enable movement in the arms and legs of a patient - surgeons would opt for DBS electrodes designed such that they would have more surface area of the electrode in contact with the respective region of the brain responsible for movement. This would result in an increased membrane potential that doesn’t decrease as linearly even as the distance from the electrode increases. For indications of mental health disorders like depression, where one would desire a slightly increased membrane potential in a localized region, surgeons would opt for a much more compact electrode that generates an increase in membrane potential localized only to that specific area of the brain.

11. Mesh Convergence

In order to understand which mesh size would be optimal for the project, six different mesh sizes were tested with respect to average temperature, as membrane potential experienced a negligible change

between meshes. Additionally, the temperature values were taken over the course of a 0.03 second period as opposed to a 1 second period in the interest of time. The configuration we ultimately decided to use for the study, as well as our mesh convergence plot, are as follows:

Table 4: The values of the element size parameters for the model's mesh configuration.

Element size parameters	Values
Maximum element size	0.27
Minimum element size	0.00101
Maximum element growth rate	1.2
Curvature factor	0.25
Resolution of narrow regions	1

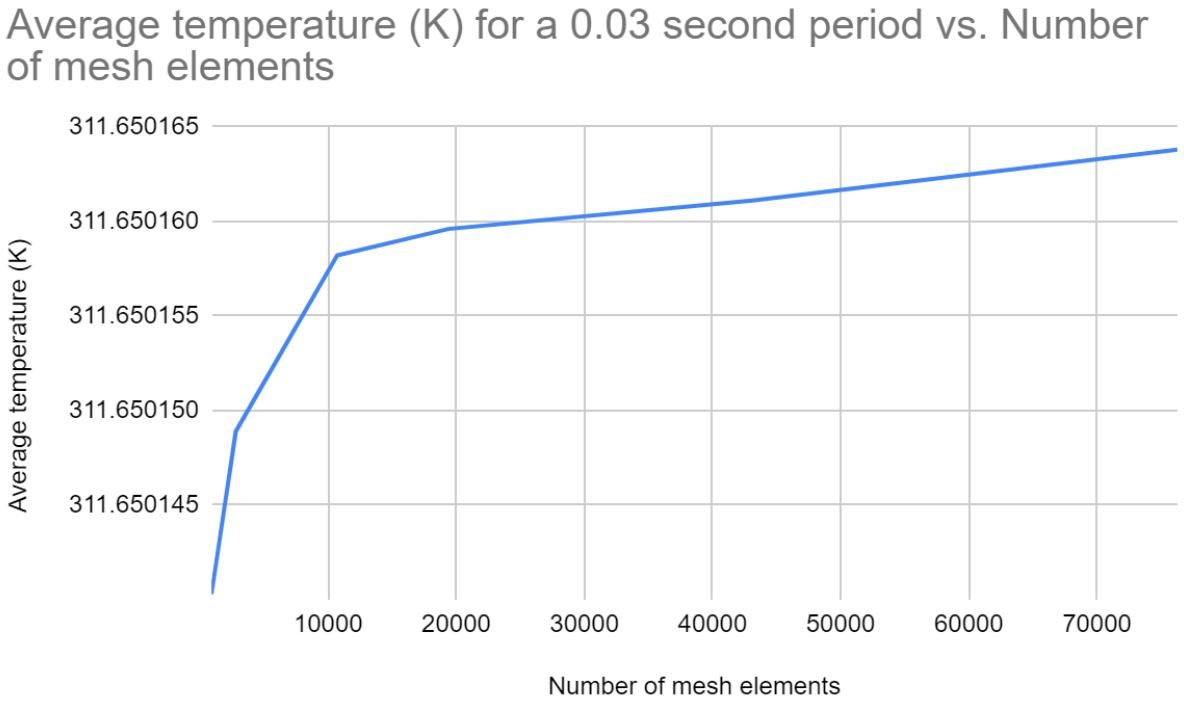

Figure 23: Plot of the mesh convergence, based on average temperature versus the number of elements.

The average temperature noticeably changes as the mesh is refined, revealing an overall increase in the temperature of the tissue with the refinement. The mesh convergence study could have been taken even further, but due to extremely long simulation times, a complete convergence was unable to be found. For this same reason, we decided to base our mesh on the extra fine mesh configuration which possessed 2788 elements, as our simulation time was already very long and we believed the accuracy of our temperature plot was satisfactory. However, if we or another group were to test our model more in the

future, we would like to use a more refined mesh, as it will provide even more accurate results than those found in this study.

12. Model Validation and Verification

The numerical results for temperature encompass a promising solution. Nonetheless, they are limited due to the fact that the time frame is smaller than the one in the paper. A time frame of 1 minute for validation was considered due to the long simulation time making a full 15-minute simulation infeasible. There is a clear upwards trend, where each pulse steadily increases the tissue's temperature, but the slope decreases as the simulation continues. The authors of this paper predicted that the waves from the electrodes would eventually cause the temperature inside of the brain to increase by 0.8 °C after 15 minutes or, when averaged out, 0.053 °C after 1 minute. This can better be understood and validated from the graph detailing the variance in temperature of the thalamic region, at a point 0.73 mm from the electrode, over a 60 second simulation period:

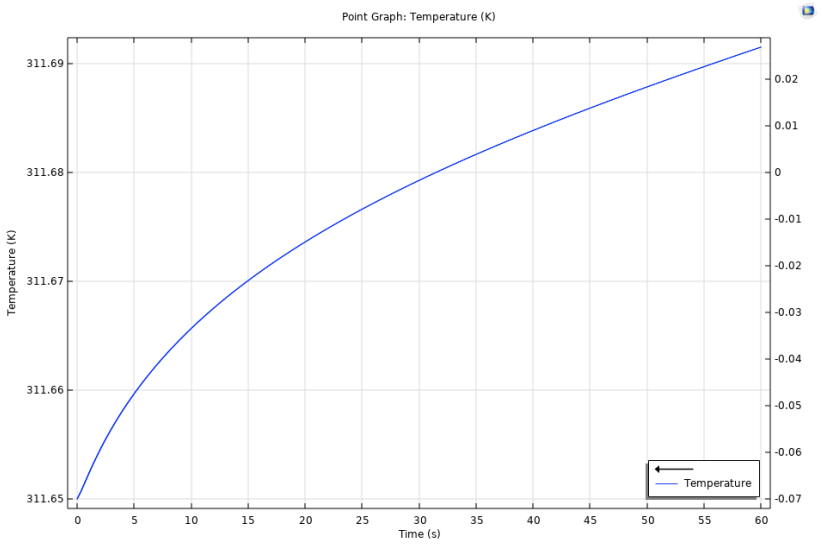

Figure 24: Variation in temperature in the thalamus over 60 seconds.

As represented in the plot, there is an evident increase in temperature from 311.65 K to 311.69 K. Even though the change in the temperature value is only by a decimal factor, this difference is important, considering that small changes in brain temperature can affect brain functionality drastically. It is assumed that if the voltage pulses from the DBS continue, then the temperature will continue to increase, based on the trend of the graph. Moreover, it was noted that after a slight upward trend of the graph initially, it follows either somewhat of a linear trend or the beginning of a plateau. This indicates that the temperature may eventually stop increasing, reaching a maximum value before maintaining steady state. Additionally, the trend, along with ***Figures 18*** and ***19***, indicate that temperature likely wouldn't keep increasing linearly with distance, but is instead localized to a region in the tissue around the electrodes. The regions of the brain far from the electrodes would not be expected to experience a noticeable increase in temperature.

The temperature change observed in 60 seconds was also concordant with the results of a similar study [16]. According to this study, a change of 0.8 °C was observed in a 15 minute simulation, and it is common in these types of studies to see temperature changes with variation in simulation parameters. Although our simulation was not run for 15 minutes, the change in temperature observed was 0.042 °C,

which is close and comparable to a 0.053 °C increase in a minute, as seen in the referred study and as seen from the graph (assuming that the trend remains the same if the model were to be simulated for a longer time). In addition, our measurement was taken for a point 0.73 mm from the electrodes, meaning that a point even closer to the electrodes is expected to increase to an even greater temperature and be even closer to the expected value.

The numerical results for the membrane potential differ significantly from the expected results, despite the patterns matching up very closely. The behavior of the membrane potential is almost exactly how it was expected to act, based on the prediction that it would act as an action potential. There is a sudden spike followed by a short hyperpolarization period and then a rest period, as shown by the following two diagrams:

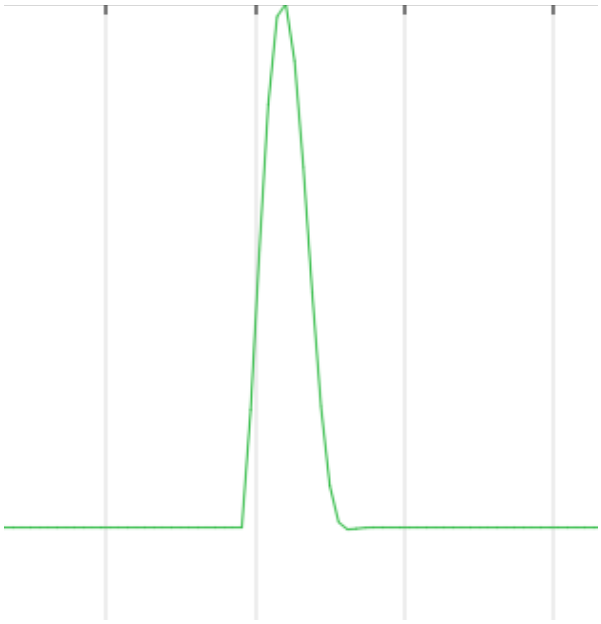

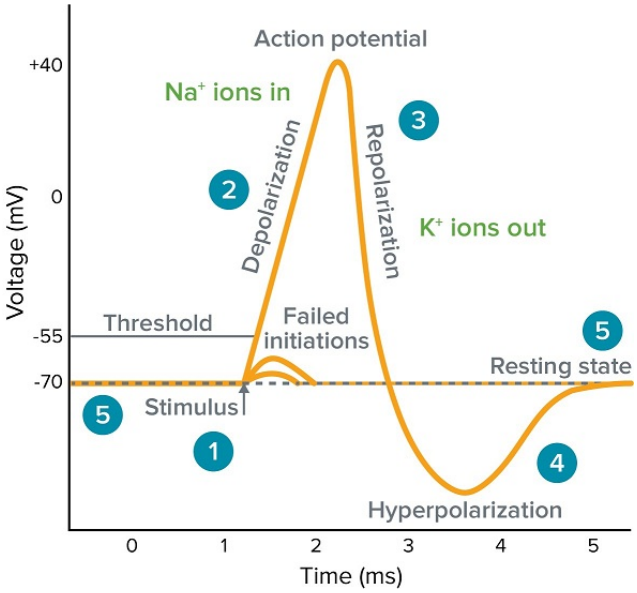

Figures 25 and 26: Graphs showing and defining the membrane potential spike and the hyperpolarization period.

Our simulation's hyperpolarization period is far less prominent than the one predicted by standard action potential behavior. This is likely either because the action potential's strength is weaker than expected, causing a weaker hyperpolarization period, or due to a calculation error by the equation solver. In the plots, at the point closest to the electrodes, the initial spike brought the membrane potential from -70 mV to +60 mV, before oscillating between -35 mV and +60 mV. However, we predicted that the membrane potential would oscillate between -70 mV and +40 mV. This leads to our numerical change in membrane potential being 95 mV compared to 110 mV, offering a possible explanation for why the hyperpolarization period is weaker. Another explanation could be that the temperature has not yet reached its expected amount of change, making its effect on the membrane potential minimal. If the simulation was run for the full 15 minutes, similar to the temperature, the numerical solution of the membrane potential could be expected to produce a result more similar to the predicted results.

13. Sensitivity Analysis

The two main variables with ranges for their values are the thermal conductivity and the input voltage. For the sensitivity analysis, these two values will be analyzed. Several simulations were performed using the parametric sweep function, varying the thermal conductivity in the thalamus from 0.53 - 0.56 W/m-K, then the thermal conductivity in the hypothalamus from 0.53 - 0.56 W/m-K, and finally, the voltage output by the electrodes from 1.0 - 2.5 V. The baseline values used were the ones used in our study: 0.53 W/m-K, 0.56 W/m-K and 1.8 V, respectively.

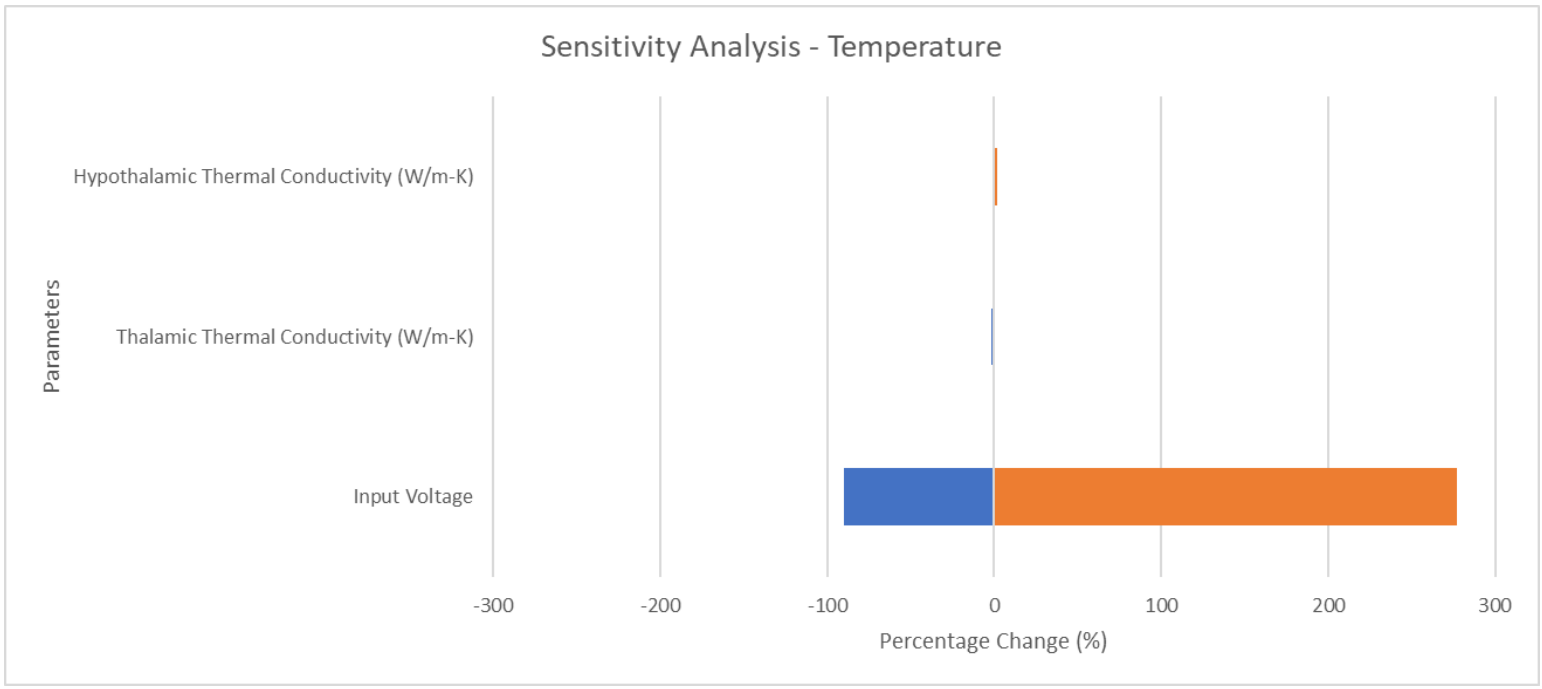

Figure 27: Sensitivity analysis plot of the temperature.

It appears changing the thermal conductivities has a negligible effect on the temperature of the tissue, barely changing it. At default, the hypothalamic thermal conductivity was 0.56 W/m-K and the thalamic thermal conductivity was 0.53 W/m-K. So, during the sensitivity analysis, it was observed how the tissue would react when these parameters were tested at the opposing values individually. The result is that increasing the thalamic thermal conductivity decreased the temperature of the tissue and decreasing the hypothalamic thermal conductivity increased the temperature of the tissue, contrary to the expectation that increasing the tissue's thermal conductivity would increase its temperature.

On the other hand, varying input voltage has a significantly larger effect on the temperature of the tissue than the thermal conductivity. Increasing the voltage from 1.8 V to 2.5 V increases the temperature by nearly 300%, supporting our previous observations. Meanwhile, setting the voltage to 1 V decreases the temperature by 90%. The massive increase in temperature from the 2.5 V input makes it completely unacceptable as an option, as it would jeopardize the patient's health.

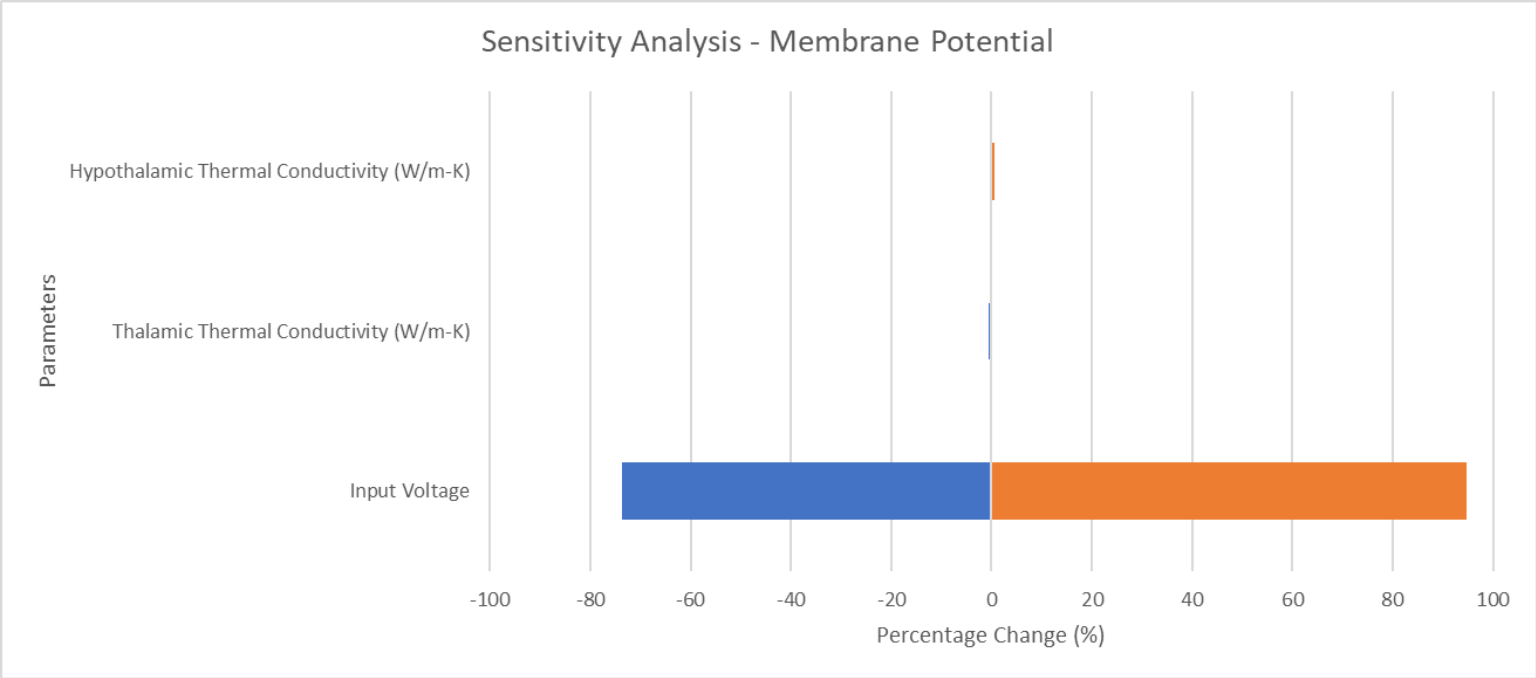

Figure 28: Sensitivity analysis plot of the membrane potential.

Similar to the temperature, varying thermal conductivity appeared to have a negligible effect on the membrane potentials of the thalamus and hypothalamus. Considering how little the thermal conductivities affect temperature within the tissues and how small of an effect the temperature has on the membrane potential, this is not very surprising and supports our previous findings.

Continuing the trends from the temperature plot, increasing the input voltage greatly increases the membrane potential of the tissue. However, the membrane potential does not experience nearly as large of an increase as the temperature, only reaching around 95%. The decrease from the 1 V input is similar, however, reaching around -75%. This sensitivity analysis provides additional support for the voltage having the most prominent effect on the membrane potential, as opposed to the temperature or thermal conductivity.

14. Conclusions and design recommendations

Various neurological and psychiatric disorders can be treated using deep brain stimulation (DBS), including Parkinson's disease, essential tremors, dystonia, and obsessive-compulsive disorder. Despite DBS's efficacy, its precise mode of operation is still not fully known. Multiple studies, including this one, investigated the changes brought about by DBS, which include an increase in temperature with time and its subsequent effect on membrane potential. Neuronal activity and metabolism are tightly regulated by brain temperature. According to our and other studies, DBS can generate localized heating in the brain, which could influence the activity of neighboring neurons. Additionally, during DBS, variations in the membrane potential of neurons have also been seen, indicating that this procedure may change how excitable the neurons in the targeted area are.

Based on the findings of this model, it was concluded that the electrical conductivity of the brain tissue has a large effect on the rate of temperature increase in the thalamus and hypothalamus. It is why the thalamus continues to increase its temperature faster than the hypothalamus, as its electrical conductivity is noticeably greater at 4.75 mS/cm compared to 4.19 mS/cm, despite having a lower thermal conductivity in our model. Ideally, the input voltage must be balanced to minimize the increase in temperature while maximizing the increase in membrane potential, so that DBS will be as effective as possible without jeopardizing the patient's health. 1.8 V indeed seems to be nearly the most ideal input voltage, increasing the membrane potential a great deal while keeping the temperature increase in the brain somewhat reasonable [15]. If the voltage is made lower, the membrane potential increase will be too low to matter, and if it's made higher, then the temperature increase will pose a risk to the health of the brain.

Additionally, the configuration of the DBS probes can considerably impact the effectiveness and safety of the procedure. The DBS probes that are currently most frequently utilized are cylinder-shaped devices with several electrodes positioned in the targeted brain region. However, the idea of more complex shapes and configurations, like directional electrodes, segmented electrodes, and multi-layered electrodes, has recently come to light. The objective of improving the design here is to achieve enhanced precision in targeting specific brain regions, the capacity to manipulate the electrical field and reduction in the spread of the current to neighboring tissue. A few design recommendations can be implemented for the following areas:

Electrode Design: Recent advances in electrode design have aimed to increase the number of electrode contacts with a radially segmented configuration to allow a horizontally directed field in multiple directions instead of one. The electric field through this new design can also be altered by utilizing anodes and cathodes to steer the direction of the electric field in the desired direction. Although new designs with multiple electrode contacts and directional advantage bring enhanced capabilities, they also lead to additional complexity in surgical implantation and pose challenges for programming the system. Heightened current amplitudes also impair the capability to mold the stimulation field in directions other than the longitudinal direction. To fully reap the rewards of novel electrode designs, programming algorithm advancements—including a move away from manual programming in favor of automated programming—will be vital.

Biocompatibility: After implantation, a temporary interaction forms between the electrode and the brain tissue. The electrical properties of the electrode-tissue interface are then determined by glial encapsulation of the electrode, protein deposition on electrode sites, and the ionic domain at the electrode-electrolyte interface [16]. Suppose stable therapeutic outcomes are to be achieved with commercial deep brain electrodes. In that case, it is essential to alleviate an inflammatory foreign body reaction, which is a general issue with the chronic placement of electrodes into the brain [17]. It is necessary for electrodes to work safely with larger charge densities in order to devise directed electrodes that stimulate smaller volumes of brain tissue. Smaller electrode sizes can be employed safely because coatings like conductive hydrogels (CHs) offer lower impedances and larger charge injection limits (CILs) than conventional platinum electrodes [18].

Implantable Pulse Generators (IPG) and Programming: In the DBS industry, IPG technology innovation has long been needed. New waveforms and patterns, programming optimization, energy

efficiency improvements, and miniaturization are required to improve therapeutic outcomes, patient safety, and comfort. DBS technology can exploit innovations already employed in Spinal Cord Stimulation. Examples include multiple independent current control, which combines unique lead contacts with a specific current source to precisely customize the size and form of the stimulation field.
One of the many methodologies being explored in the arena of neurostimulation is the optimization of programming through standardization. Both BurstDR and HF-10 utilize standardized algorithms, which replace the occasionally time-consuming and laborious coding with simplicity [19]. With the ultimate objective of closed feedback loops and programming optimization which is intelligence-based, this methodology will likely find its way into DBS programming.

Stimulation can be modified in response to disease-specific neural biomarkers using closed-loop DBS systems that simultaneously store and modulate brain activity. Open-access software can be utilized to identify DBS electrodes and simulate the volume of tissue activated surrounding the electrodes based on the stimulation parameters, providing insight into essential neurocircuitry elements and remote programming by doctors will be available as DBS systems become wireless network compatible. Through these suggestions, the goal is to contribute to making Deep Brain Stimulation more accurate, less invasive, safer, and effective and ensure that it will be used on a more significant percentage of patients for whom other treatments have proven ineffective.

15. Regulatory Compliance and Overview on Neuromodulation Devices

When a novel medical device has been developed and is introduced to the market, regulatory compliance forms the pathway for market commercialization and cannot be overlooked. Regulatory compliance ensures that the device is "regulated," that is, it is safe, effective, and manufactured under appropriate quality control measures. In a few cases/classes of medical devices, data from clinical trials is mandatory to establish this safety and efficacy, and establish that the device's function aligns with its intended use. This not only protects patient safety, but also helps ensure compliance with legal requirements and can provide access to federal reimbursement pathways such as Medicare and Medicaid. In addition, obtaining regulatory clearance or approval gives the device a competitive advantage over other manufacturers in the market by demonstrating its quality and reliability.

The probe, electrode, and implantable pulse generator form the instrumentation required for DBS, and are grouped under neuromodulation devices by the FDA. This is a class 3 medical device, a category reserved for high-risk devices that are directly in contact with the patient and are usually intended for critical conditions for sustaining life. For these reasons, they require the most stringent regulatory and quality control frameworks. FDA also requires the manufacturers of these devices to conduct post-market surveillance of their devices following launch to ensure patient safety. However, given the extent of invasiveness of the device, the degree of heating caused inside the brain, and the potential side-effects, DBS has long been a controversial procedure and the FDA has received approximately 600 adverse event reports till date from patients following implantation of the device.

References

[1] Hariz ML, Blomstedt P, Zrinzo L. (2010) Deep brain stimulation between 1947 and 1987: The untold story. Neurosurgical Focus 29(2): E1. https://thejns.org/focus/view/journals/neurosurg-focus/29/2/2010.4.focus10106.xml

[2] Gardner J. A history of deep brain stimulation: Technological innovation and the role of clinical assessment tools. Soc Stud Sci. 2013 Oct;43(5):707–28. doi: 10.1177/0306312713483678. PMCID: PMC3785222.

[3] Kahan, Joshua, et al. "The safety of using body-transmit MRI in patients with implanted deep brain stimulation devices." *PLoS One* 10.6 (2015): e0129077.

[4] M. M. Elwassif, Q. Kong, M. Vazquez and M. Bikson, "Bio-Heat Transfer Model of Deep Brain Stimulation Induced Temperature changes," 2006 International Conference of the IEEE Engineering in Medicine and Biology Society, New York, NY, USA, 2006, pp. 3580-3583, doi: 10.1109/IEMBS.2006.259425.

[5] Baysal U, J Haueisen. Use of a priori information in estimating tissue resistivities-application to human data in vivo. Physiol. Meas. 2004; 25: 737-748.

[6] Xiaojiang X, P Tikuisis and G Giesbrecht. A mathematical model for human brain cooling during cold-water near-drowning. Journal of Applied Physiology 86:265-272, 1999.

[7] Alonso, Fabiola, et al. "Investigation into deep brain stimulation lead designs: a patient-specific simulation study." Brain sciences 6.3 (2016): 39.

[8] Jabbari, M.B., Karamati, M.R. The effects of temperature on the dynamics of the biological neural network. J Biol Phys 48, 111–126 (2022). https://doi.org/10.1007/s10867-021-09598-1

[9] Maldonado, Charli A., Brittney D. Wooley, and Joseph J. Pancrazio. "The excitatory effect of temperature on the Hodgkin-Huxley model." The Premier Undergraduate Neuroscience Journal.[interaktyvus] (2015).

[10] Jabbari, Mohammad B., and Mahdi Rezaei Karamati. "The effects of temperature on the dynamics of the biological neural network." Journal of Biological Physics 48.1 (2022): 111-126.

[11] Hongsheng Sun, Haoran Chen, Yu Chen et al. Thermal conductivity of binary Platinum-Iridium alloys, 01 August 2022, PREPRINT (Version 1) available at Research Square [https://doi.org/10.21203/rs.3.rs-1896205/v1]

[12] InformedHealth.org [Internet]. Cologne, Germany: Institute for Quality and Efficiency in Health Care (IQWiG); 2006-. How is body temperature regulated and what is fever? 2009 Jul 30 [Updated 2016 Nov 17]. Available from: https://www.ncbi.nlm.nih.gov/books/NBK279457/

[13] C. Gabriel. Compilation of the Dielectric Properties of Body Tissues at RF and Microwave Frequencies- Low Frequency Conductivity. Report N.AL/OE-TR- 1996-0037, Occupational and environmental health directorate, Radiofrequency Radiation Division, Brooks Air Force Base, Texas (USA), 1996. It-is Foundation. Available from: https://itis.swiss/virtual-population/tissue-properties/database/low-frequency-conductivity/

[14] It-is Foundation. Compilation of the Dielectric Properties of Body Tissues at RF and Microwave Frequencies- Database Summary. 2010-2022. Available from: https://itis.swiss/virtual-population/tissue-properties/database/database-summary/

[15] Steven Streatfield Gill, Deep Brain Stimulation. (2005) United States Patent Application Publication. Available at: https://patents.google.com/patent/US20060058855A1/en

[16] Kronenburger M, Nolte KW, Coenen VA, Burgunder JM, Krauss JK, Weis J. Brain alterations with deep brain stimulation: New insight from a neuropathological case series. Mov Disord. 2015 Jul;30(8):1125-30. doi: 10.1002/mds.26247. Epub 2015 May 23. PMID: 26011773.

[17] Moss J, Ryder T, Aziz TZ, Graeber MB, Bain PG. Electron microscopy of tissue adherent to explanted electrodes in dystonia and Parkinson's disease. Brain. 2004 Dec;127(Pt 12):2755-63. doi: 10.1093/brain/awh292. Epub 2004 Aug 25. PMID: 15329356.

[18] Krauss, J. K., Lipsman, N., Aziz, T., Boutet, A., Brown, P., Chang, J. W., Davidson, B., Grill, W. M., Hariz, M. I., Horn, A., Schulder, M., Mammis, A., Tass, P. A., Volkmann, J., & Lozano, A. M. (2021). Technology of deep brain stimulation: current status and future directions. *Nature reviews. Neurology*, *17*(2), 75–87. https://doi.org/10.1038/s41582-020-00426-z

[19] Kapural L, Yu C, Doust MW, Gliner BE, Vallejo R, Sitzman BT, Amirdelfan K, Morgan DM, Brown LL, Yearwood TL, Bundschu R, Burton AW, Yang T, Benyamin R, Burgher AH. Novel 10-kHz High-frequency Therapy (HF10 Therapy) Is Superior to Traditional Low-frequency Spinal Cord Stimulation for the Treatment of Chronic Back and Leg Pain: The SENZA-RCT Randomized Controlled Trial. Anesthesiology. 2015 Oct;123(4):851-60. doi: 10.1097/ALN.0000000000000774. PMID: 26218762.